



## ELM propagation and fluctuations characteristics in H- and L-mode SOL plasmas on JT-60U

Nobuyuki Asakura<sup>1)</sup>

**N.Ohno**<sup>2)</sup>, **H.Kawashima**<sup>1)</sup>, **H.Miyoshi**<sup>3)</sup>, **G.Matsunaga**<sup>1)</sup>,  
**N.Oyama**<sup>1)</sup>, **S.Takamura**<sup>3)</sup>, **Y.Uesugi**<sup>4)</sup>, **M.Takechi**<sup>1)</sup>,  
**T.Nakano**<sup>1)</sup>, **H.Kubo**<sup>1)</sup>

<sup>1)</sup>Japan Atomic Energy Agency, Naka

<sup>2)</sup>EcoTopia Science Institute, Nagoya Univ., Nagoya

<sup>3)</sup>Graduate School of Engineering, Nagoya Univ., Nagoya

<sup>4)</sup>Faculty of Engineering, Kanazawa Univ., Kanazawa

# CONTENTS

---

- 1. Introduction: ELM and fluctuation study**
- 2. Parallel and Radial propagation of ELM in Low-Field-Side SOL**
- 3. ELM propagation in High-Field-Side SOL**
- 4. Fluctuation characteristics by statistic analysis**
- 5. Summary and conclusion**

# 1. ELM and fluctuation study in SOL and divertor

- Understanding of **ELM dynamics** is important to evaluate **transient heat and particle loadings to the first wall** as well as **the divertor**:  
ELM plasma propagation **along** and **perpendicular to the field lines** was investigated at **High-** and **Low-field-side SOLs**.
- Fluctuation characteristics (non-diffusion/bursty events) of SOL plasma were studied in ELMy H-and L-modes, using statistic analysis.

## Main SOL/divertor diagnostics:

### (1) Probe measurement (500kHz sample):

Ion flux ( $j_s$ ) and floating potential ( $V_f$ )  
at 3 poloidal locations and divertor target

### (2) Fast TV camera (6-8kHz)

$D_\alpha$  emission image in divertor

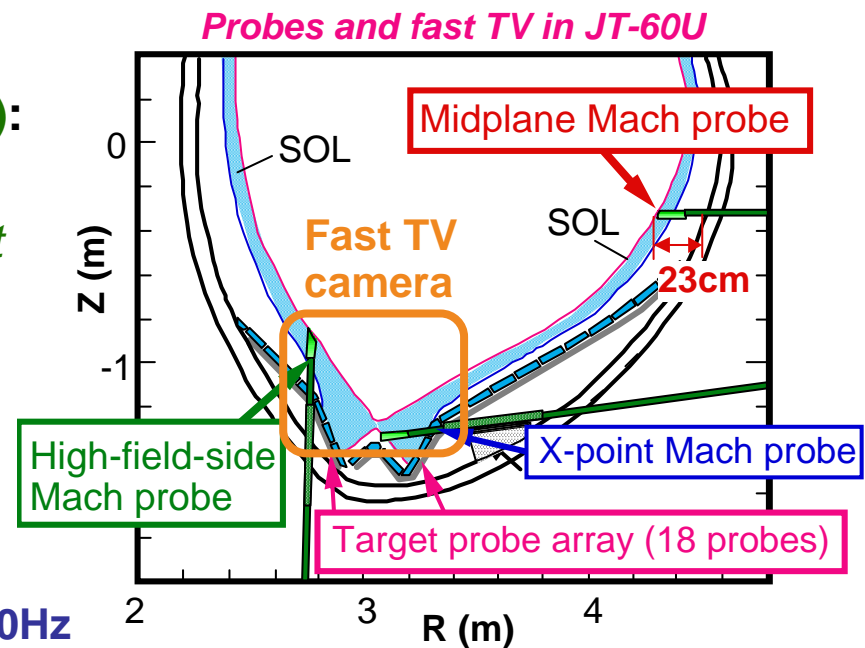
**All sampling clocks are synchronized.**

## ELMy H-mode plasma:

$I_p=1\text{MA}$ ,  $B_t=1.87\text{T}$ ,  $P_{\text{NB}}=5.5\text{MW}$

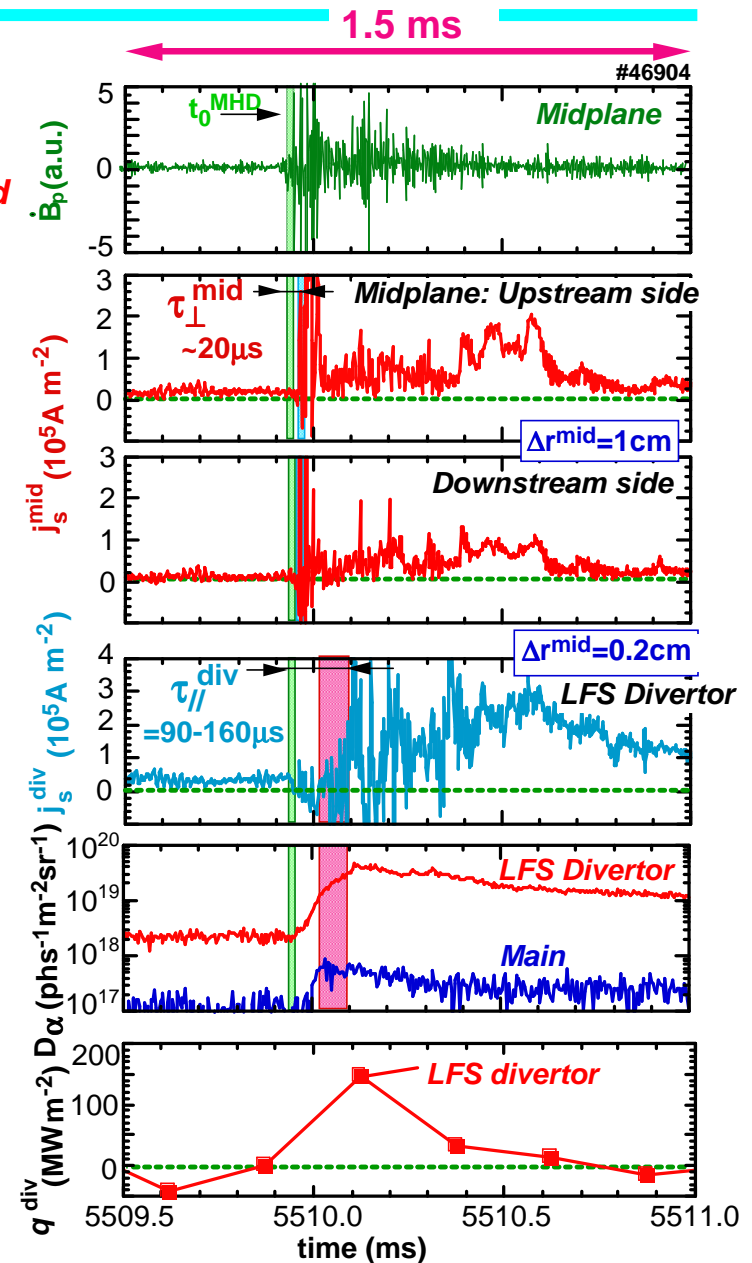
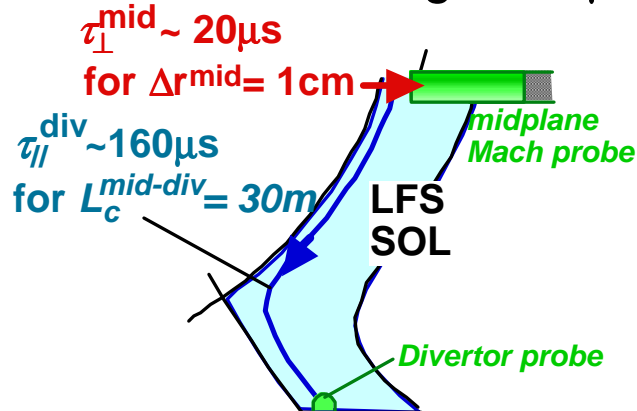
$n_e=1.8\text{-}2.1\times 10^{19}\text{m}^{-3}$  ( $n_e/n^{\text{GW}}=0.5\text{-}0.54$ ),  $f_{\text{ELM}}\sim 20\text{-}40\text{Hz}$

$T_e^{\text{ped}}\sim 700\text{ eV}$ ,  $T_i^{\text{ped}}\sim 900\text{ eV}$ ,  $\Delta W^{\text{ELM}}/W^{\text{ped}}=10\text{-}12\%$



# 2. Parallel and Radial propagation of ELM in LFS SOL

- Plasma is exhausted at *large*  $B_p$  turbulence  
 $\Rightarrow$  start of first large  $B_p$  peak:  $t_0^{MHD}$  is defined.
- **Plasma flux at midplane Mach probe:  $j_s^{mid}$**   
*Large peaks appear during  $B_p$  turbulence*  
 $\Rightarrow$  ELM plasma reaches *Both sides* of Mach probe:  $\tau_{\perp}^{mid}$  ( $\sim 20\mu s$ )
- **Plasma flux at LFS divertor:  $j_s^{div}$**   
*starts increasing after large  $B_p$  turbulence*  
 $\Rightarrow$  ELM flux reaches divertor:  $\tau_{\parallel}^{div}$  ( $90-160\mu s$ )  
*which is comparable to parallel convection time:*  
 $\tau_{\parallel}^{conv} = L_c^{mid-div} / C_s^{ped} (2.7 \times 10^5 \text{ m/s}) \sim 110\mu s.$   
 $\Rightarrow j_s^{div}$  *base-level* increases during  $\sim 500\mu s$ .



# Radial propagation of ELM towards the first wall

Magnetic turbulence and  $D_\alpha$  increase start almost simultaneously

⇒  $j_s^{mid}$ : **large peak and/or “multi-peaks”**  
with **large  $\delta V_f$**  ( $\sim 800V$ ):  $T_e, T_i \sim$  a few 100eV  
(peak duration:  $\delta t_{peak} = 10-25\mu s$ )

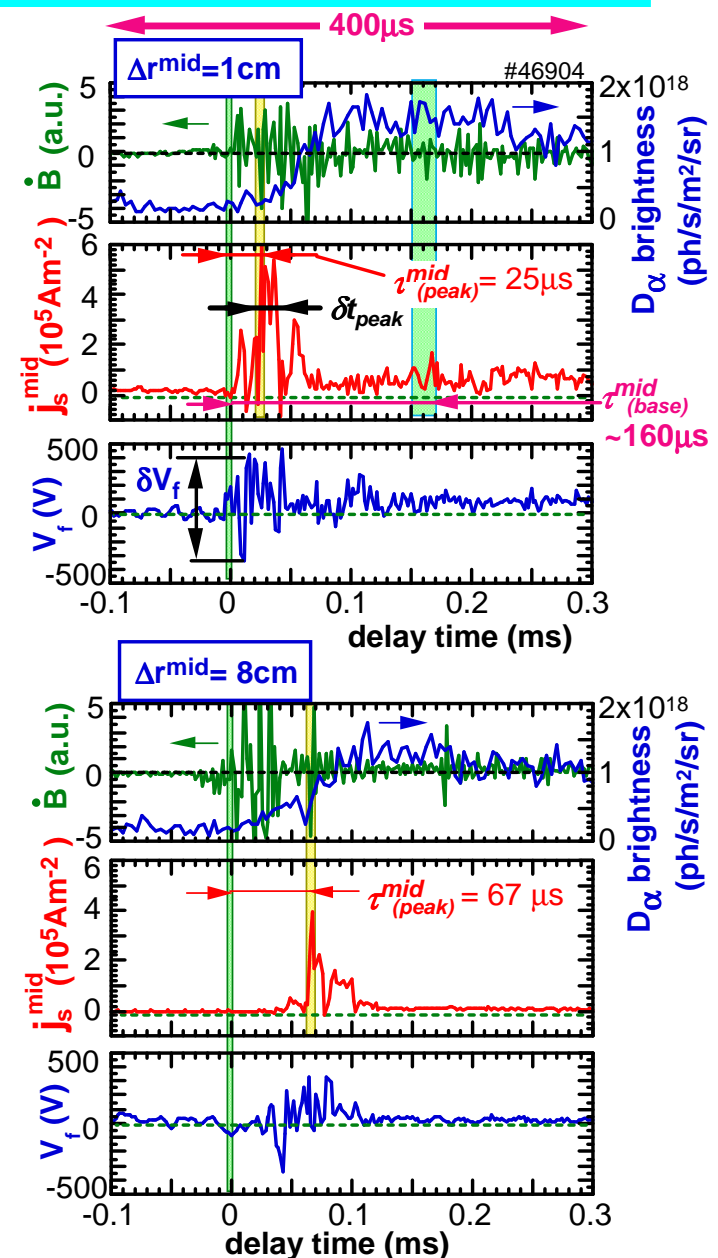
⇒ “base-level” of  $j_s^{mid}$  increases:

base-level enhancement time,  $\tau_{\perp}^{mid}(base)$ ,  
is larger than parallel convection time,  $\tau_{\parallel}^{conv}$   
( $\sim 110\mu s$ ).

- **Delay of  $j_s^{mid}$  peak:  $\tau_{\perp}^{mid}(peak)$**   
increases with  $\Delta r^{mid}$  in near-SOL.  
-- Delay of large  $\delta V_f$  is also observed.

⇒  $j_s^{mid}$  **peak propagates towards first wall,**  
faster than **parallel convection:**

$$\tau_{\perp}^{mid}(peak) < \tau_{\parallel}^{conv} \sim \tau_{\parallel}^{div} \leq \tau_{\perp}^{mid}(base)$$



# Radial distribution of ELM plasma

**Peak particle flux,  $j_s^{mid}(peak)$ : 20-50 times larger than  $j_s^{mid}$  btw. ELMs**

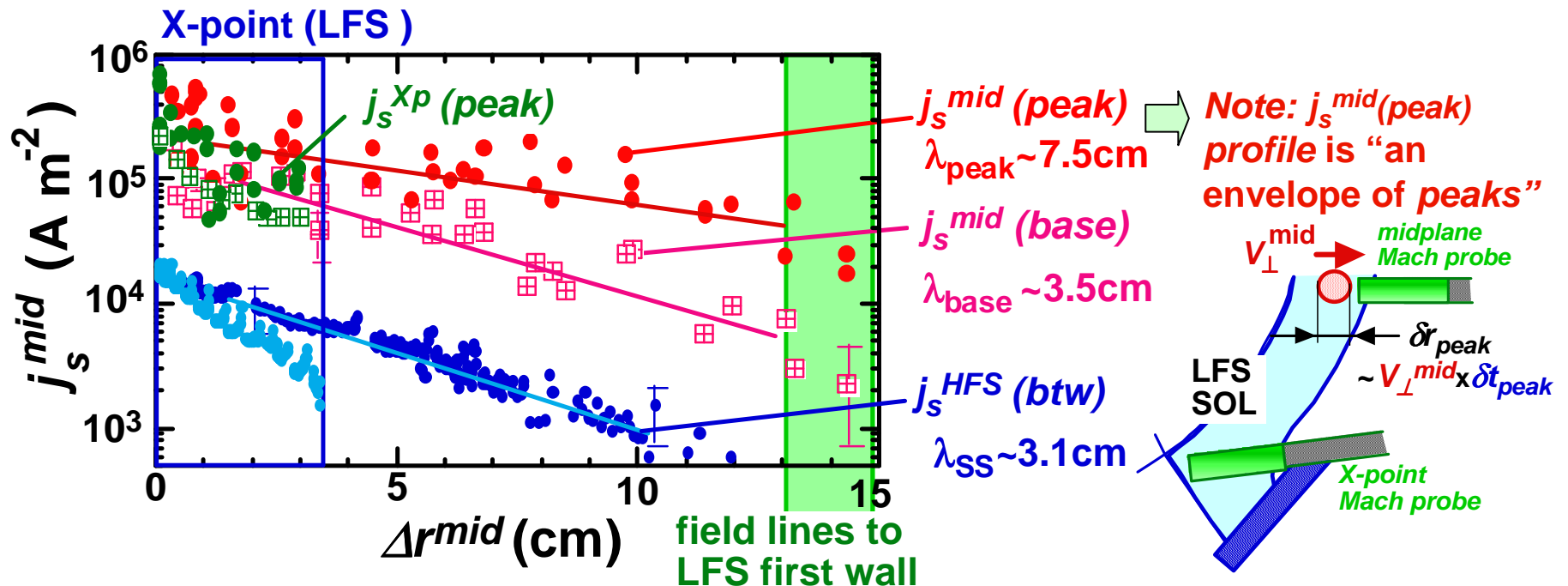
$j_s^{mid}(peak)$  propagates up to the first wall shadow ( $\Delta r^{mid} > 13\text{cm}$ )

with large decay length:  $\lambda_{peak} \sim 7.5\text{cm}$  ( $\sim 2.5 \times \lambda_{SS} \sim 3\text{cm}$ )

**Max. base-level,  $j_s^{mid}(base)$ : 10-20 times larger than  $j_s^{mid}$  btw. ELMs**

Decay length of  $j_s^{mid}(base)$  is comparable to  $\lambda_{SS}$ .

**Peak particle flux near X-point,  $j_s^{Xp}(peak)$ , is reduced.**



# Propagation velocity of ELM particle flux

- Delay of peak particle flux,  $j_s^{mid}(peak)$ :  $\tau_{\perp}^{mid}(peak)$  increases with  $\Delta r^{mid}$  at near-SOL (< 5cm)

⇒ Average radial velocity:

$$V_{\perp}^{mid}(peak) = \Delta r^{mid} / \tau_{\perp}^{mid}(peak) = 0.4-1.5 \text{ km/s}$$

Radial scale of peak is estimated:

$$\delta r_{peak} = V_{\perp}^{mid}(peak) \times \delta t_{peak} (10-25 \mu\text{s}) \sim 0.5-4 \text{ cm}$$

Characteristic length of radial propagation

(during *parallel convection time*):

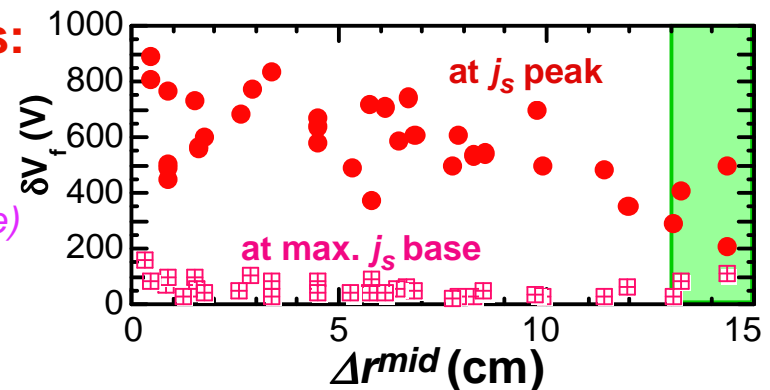
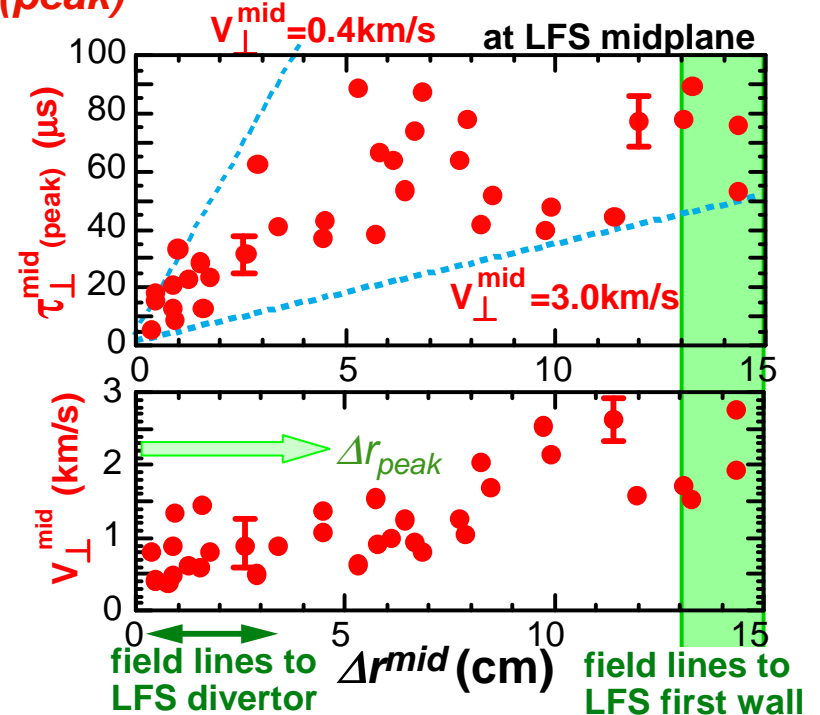
$$\Delta r_{peak} = V_{\perp}^{mid}(peak) \times \tau_{\parallel}^{conv} = 4-15 \text{ cm}$$

- ⇒ Peak particle flux (temperature of a few 100eV) reaches LFS Baffle or First wall.

At far-SOL ( $\Delta r^{mid} > 6 \text{ cm}$ ),  $\tau_{\perp}^{mid}(peak) = 40-90 \mu\text{s}$ :

$V_{\perp}^{mid}(peak) = 1.5-3 \text{ km/s}$  becomes faster.

- Delay of base-level flux,  $j_s^{mid}(base)$ :  $\tau_{\perp}^{mid}(base)$  is ranged in 100-300  $\mu\text{s}$  with low  $V_f (< 150 \text{ V})$ .
- ⇒ heat load is small due to low  $T_e$  &  $T_i$ .



# 3. ELM propagation in High-Field-Side SOL

$D_\alpha$  increase start almost simultaneously both at HFS and LFS divertors

**Enhancement of  $j_s^{HFS}$  base-level and SOL flow towards HFS divertor** are observed after parallel convection time from LFS to HFS:

$$\tau_{||}^{conv} = L_c^{LFS-HFS}(50m)/C_s^{ped} \sim 185 \mu s$$

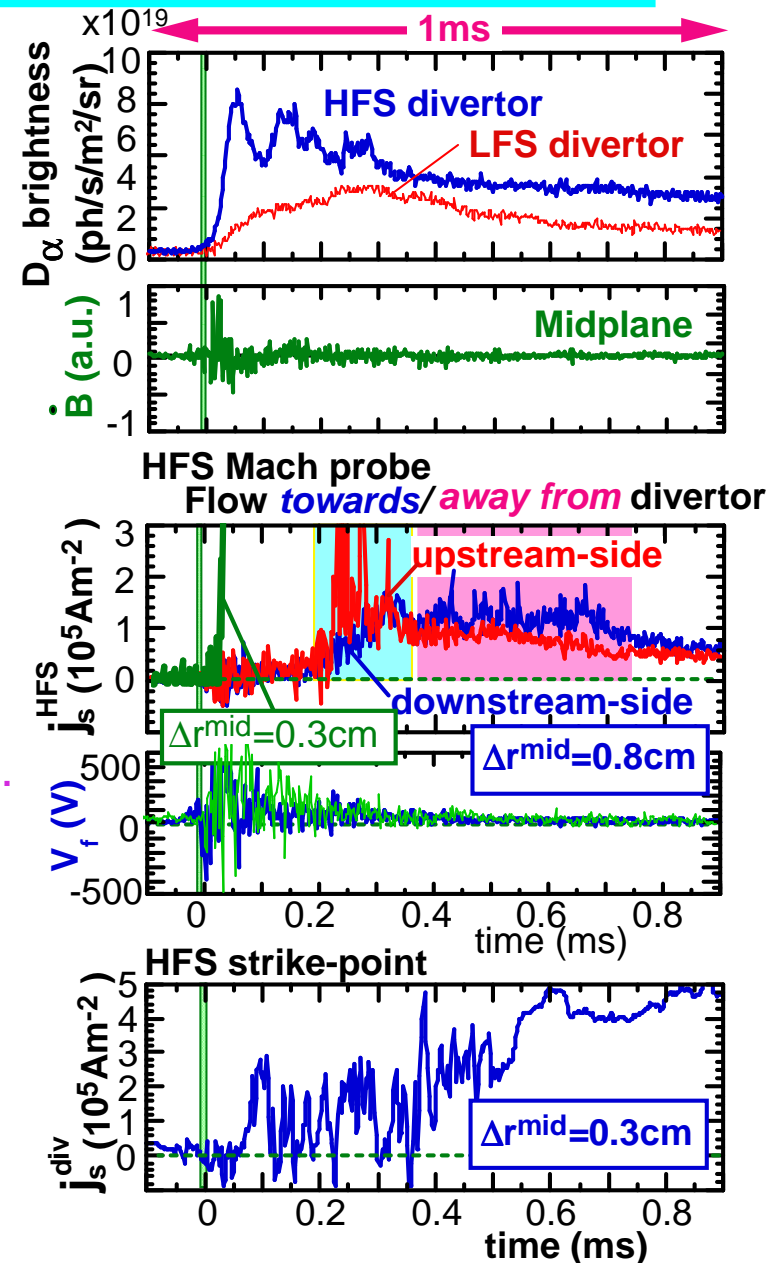
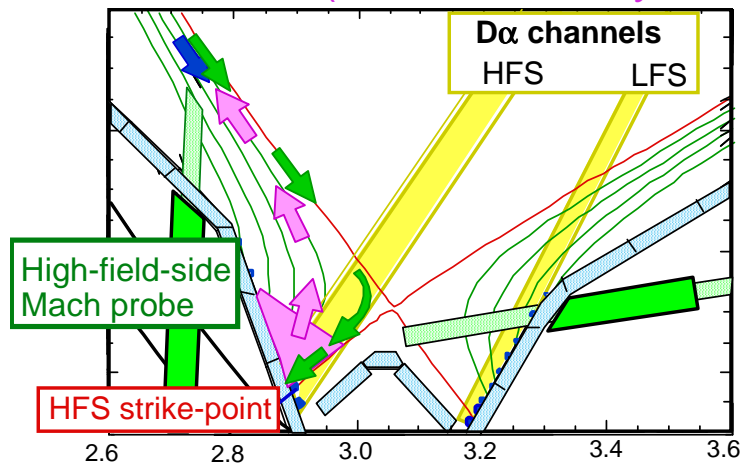
⇒ **Parallel convection towards HFS divertor**

**Only near separatrix ( $\Delta r^{mid} < 0.3cm$ ), fast  $j_s^{HFS}$  and/or heat load to Mach probe is measured:**

heat flux may be carried by fast el./ conduction

⇒ neutrals are released at target due to  $T_w$  rise.

⇒ **"flow reversal"** (SOL flow away from divertor).





# Radial distribution of ELM plasma in HFS SOL

- Conductive heat flux/ fast electrons may be transported **near separatrix**.

- Large peaks are observed occasionally:**

$j_s^{HFS}(peak)$  and  $\delta V_f$  (~100V) are smaller than those in **LFS SOL**.

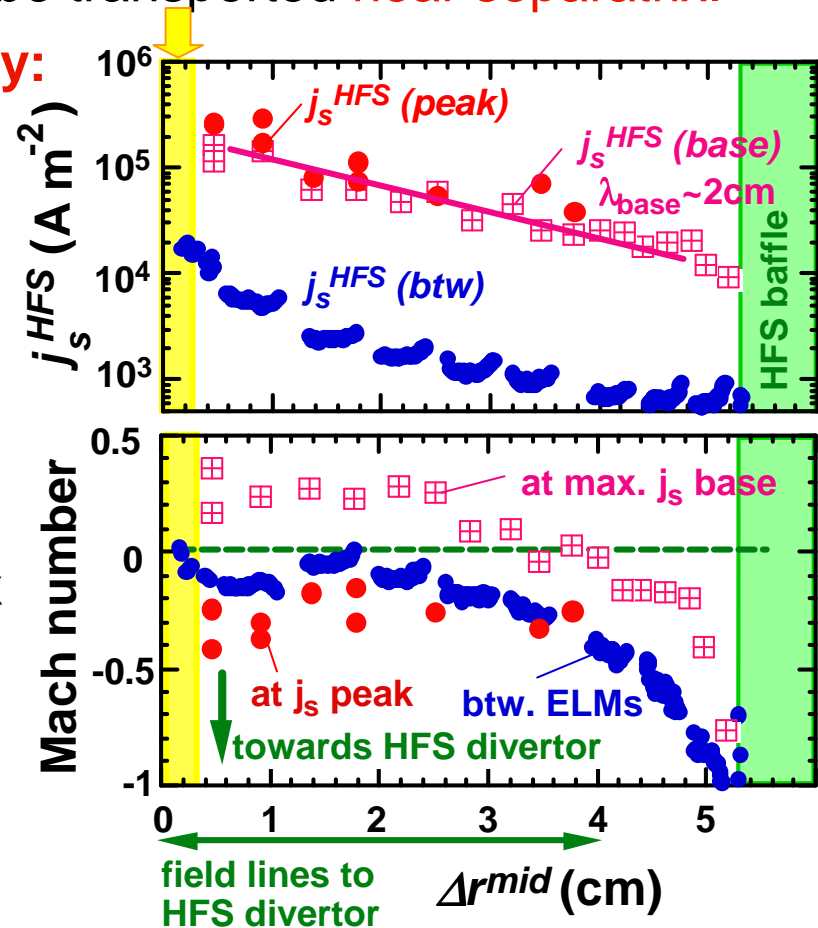
Fast SOL flow ( $M_{//}$  up to 0.4) is produced towards HFS divertor.

**Parallel convection from LFS to HFS.**

- $j_s^{HFS}(base)$  **enhancement** near separatrix is comparable to that in **LFS SOL**, while **HFS  $\lambda_{base}$  (~2cm)** is smaller than **LFS  $\lambda_{base}$  (~3.5cm)**.

**"SOL flow reversal"** is generated over wide area in HFS SOL ( $\Delta r^{mid} < 3.5cm$ ):

Large influence of neutrals may be caused by conductive heat flux/ fast electrons.



# Filament-like image is observed in LFS divertor

Fast TV (up to 8kHz) views divertor from tangential port:

HFS divertor:

$D_\alpha$  emission is enhanced immediately  $\Rightarrow$  Flow reversal is generated.

LFS divertor:

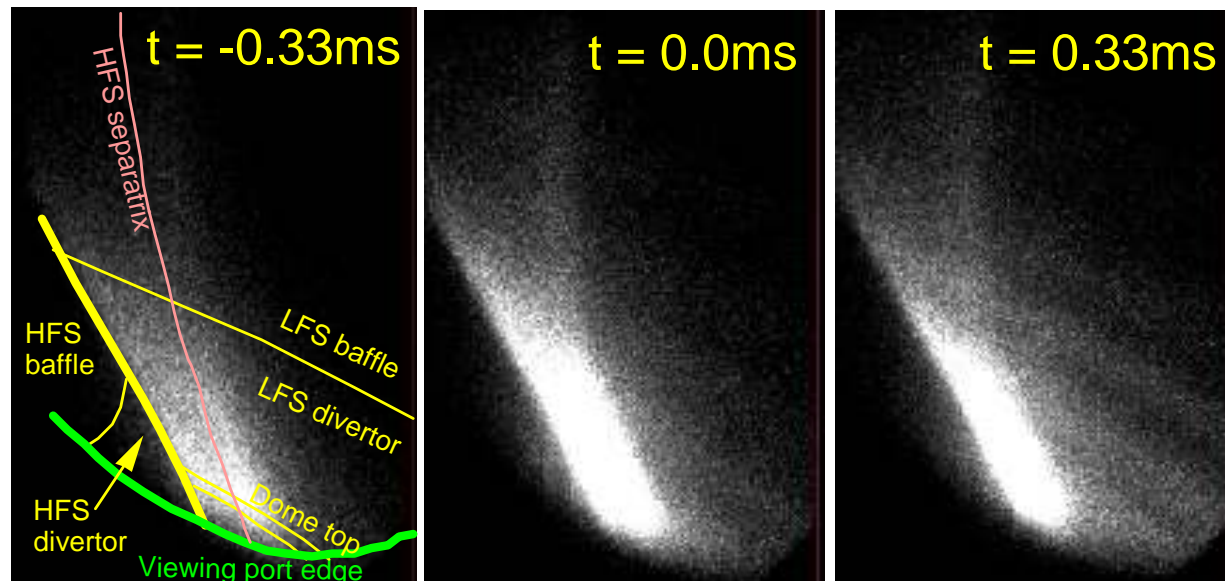
3-4 filament-like structures are observed above divertor and baffle for  $\sim 1$  ms.

Radial scale of the filament:  $\delta r \sim 3-5$  cm

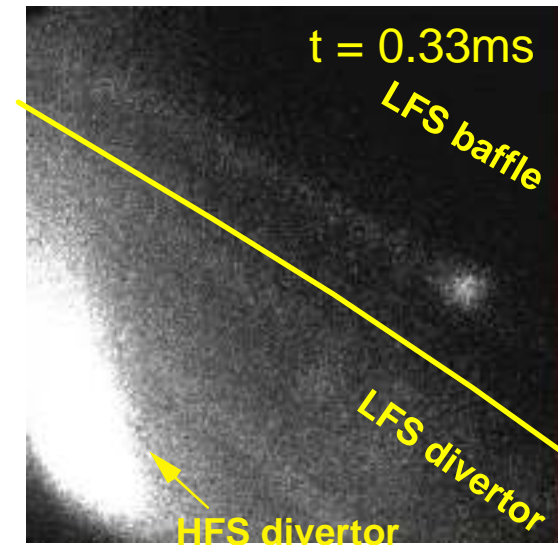
**Particle flux is deposited locally, but extended over wide area:**

**LFS baffle as well as divertor plate**

Viewing Divertor region tangentially (512x1025 pixels, 3kHz)

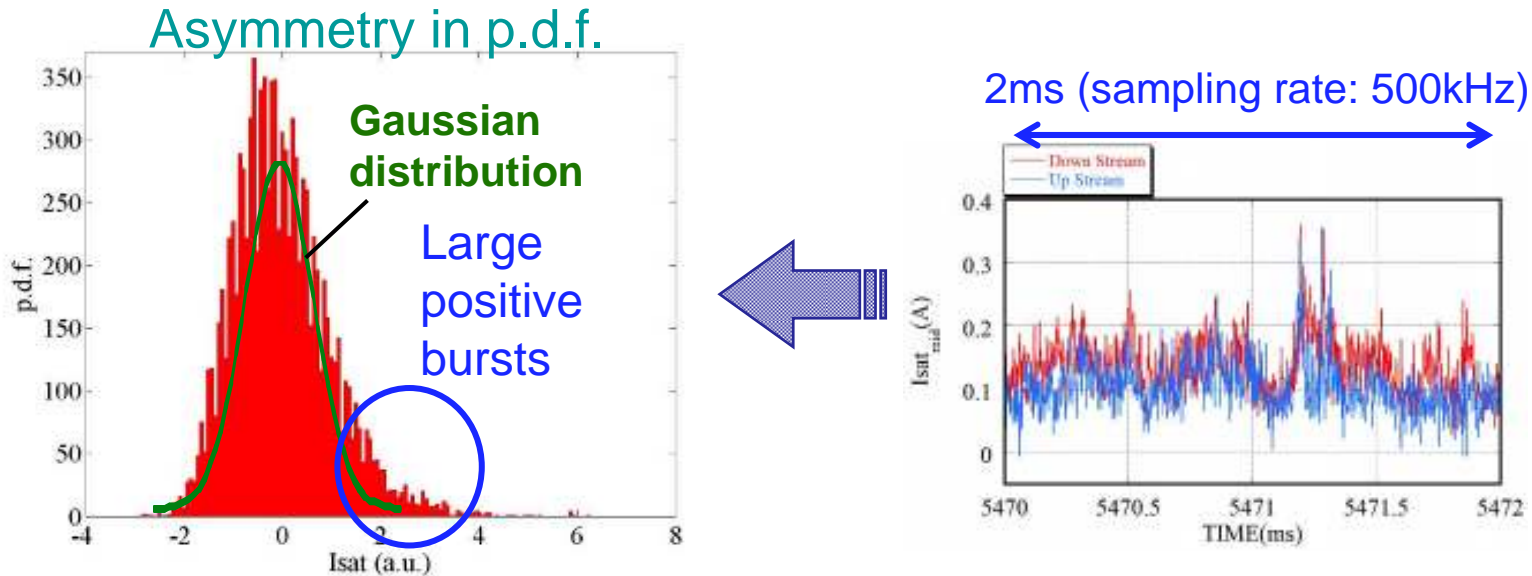


(512x512 pixels, 6kHz)



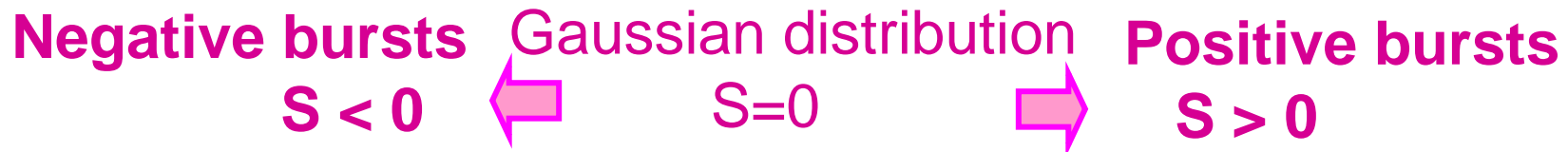
# 4. Fluctuation characteristics by statistic analysis

Probability Distribution Function (p.d.f.) is applied to  $j_s$  fluctuations  
*Between ELMs in H-mode* and *L-mode* plasmas



p.d.f. moment represents fluctuation property different from random:

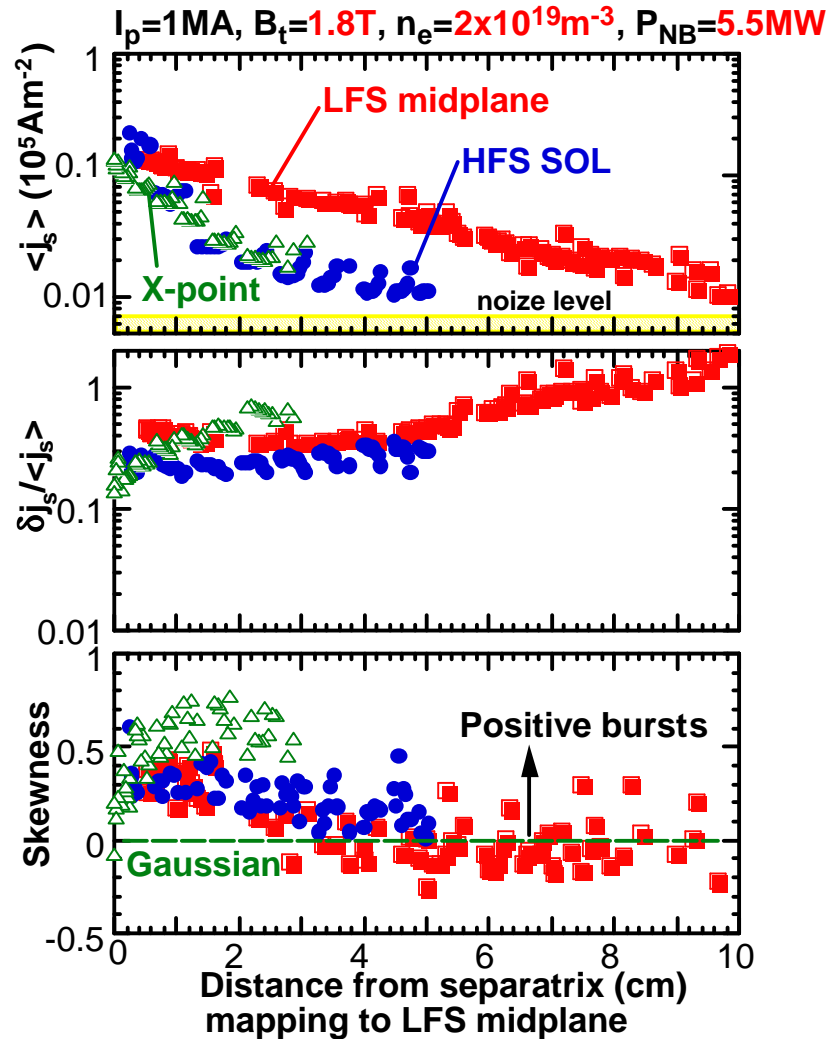
normalized 3rd moment: Skewness =  $\langle x^3 p \rangle / \langle x^2 p \rangle^{3/2}$   $\leftrightarrow$  asymmetry in p.d.f.



# Fluctuation property is different in H- and L-modes

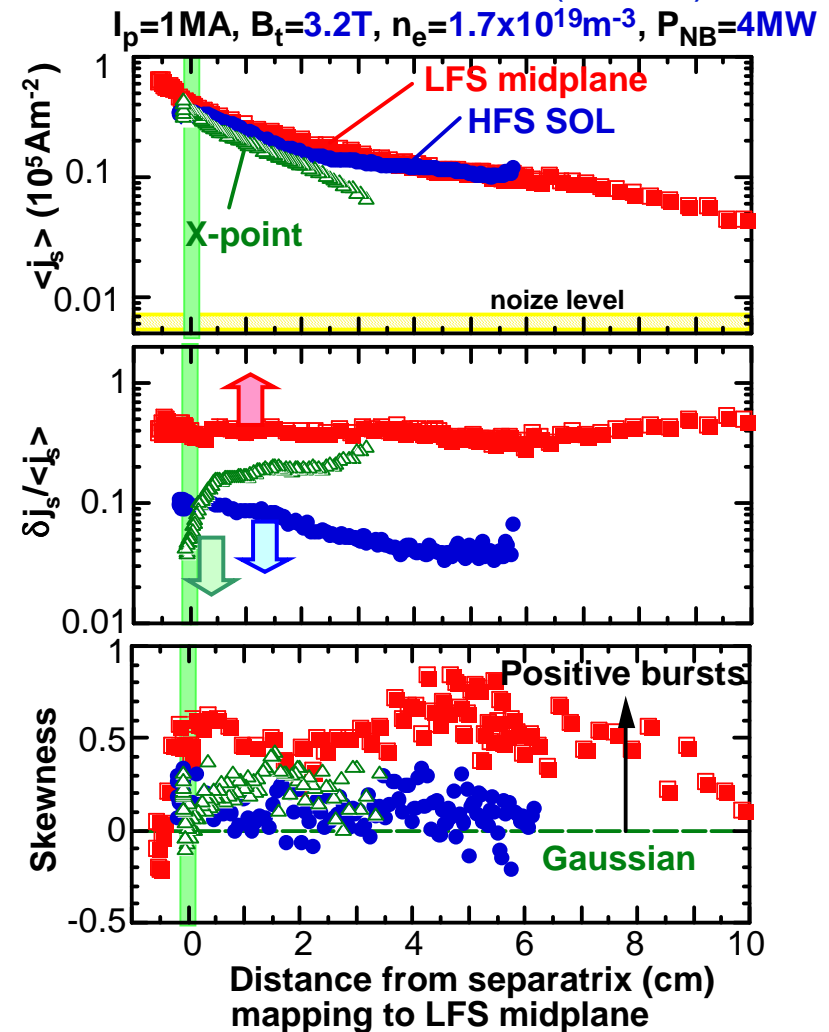
## ELMy H-mode (between ELMs):

$\delta j_s / \langle j_s \rangle$  near separatrix (20-30%) is similar.  
 bursty events are localized near-SOL (<3cm).



## L-mode:

Large asymmetry in  $\delta j_s / \langle j_s \rangle$ : 30~40% at LFS midplane, and bursty events extend to far-SOL (<10cm).



# 5. Summary and conclusions

---

Time scale and radial distribution of ELM propagation for Type-1 ELM ( $f_{ELM} = 20-40$  Hz) were investigated **at HFS and LFS SOLs** with synchronizing sampling-clocks.

**(1) ELM peak heat/particle flux appeared dominantly at LFS midplane:**

*Large  $j_s^{mid}$  peaks (high  $V_f$ ) propagated towards first wall with  $V_{\perp}^{mid} = 1.5-3$  km/s:  $\tau_{\perp}^{mid} (= 40-90\mu s)$  was faster than parallel convection to divertor ( $\sim 110\mu s$ ).  
 $\Rightarrow$  fast peak flux (with a few 100eV) will cause local heat and particle loadings.*

**(2) ELM heat and particle flux in HFS SOL and divertor:**

*Fast heat/particle transport was seen **near separatrix** ( $\Delta r^{mid} < 0.4\text{cm}$ ) maybe by conduction/ fast electrons  $\Rightarrow$  producing large neutral desorption and **flow reversal**.  
**Convective flux** was transported towards HFS divertor, but small heat deposition.*

**(3) Fluctuations Between ELMs: statistical analysis (P.D.F.) determined**

$\delta j_s / \langle j_s \rangle$  (20-30%) was comparable at three poloidal positions  
 $\Rightarrow$  **bursty events are localized in near-SOL** ( $\Delta r^{mid} < 3$  cm). **On the other hand,** in L-mode, **bursty events extend to far-SOL** ( $\Delta r^{mid} < 10\text{cm}$ ) only at LFS Midplane.

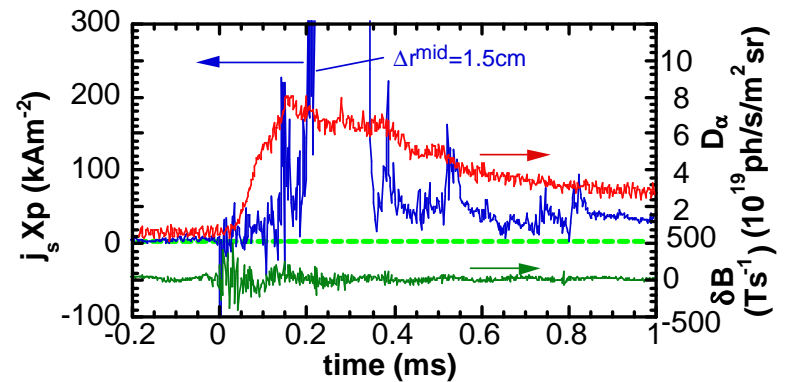
Measurements for fast deposition of ELM heat flux and wide 2D view on the first wall and divertor will improve evaluation of power load deposition on PFC.

# Filament-like image is observed in LFS divertor

Fast TV (up to 8kHz) views divertor from tangential port:

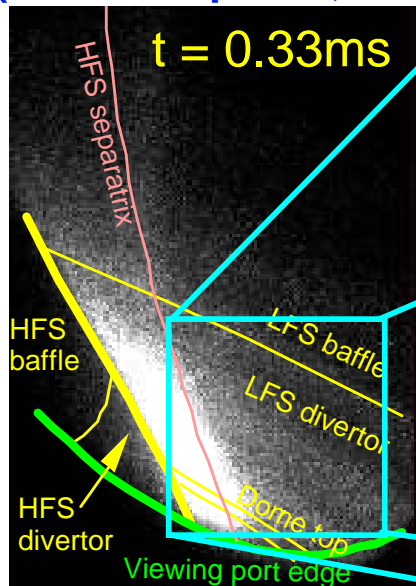
LFS divertor:

3-4 filament-like structures are observed above divertor and baffle plates during  $\sim 1$  ms.  
 Radial scale of the filament:  $\delta r \sim 3-5$  cm

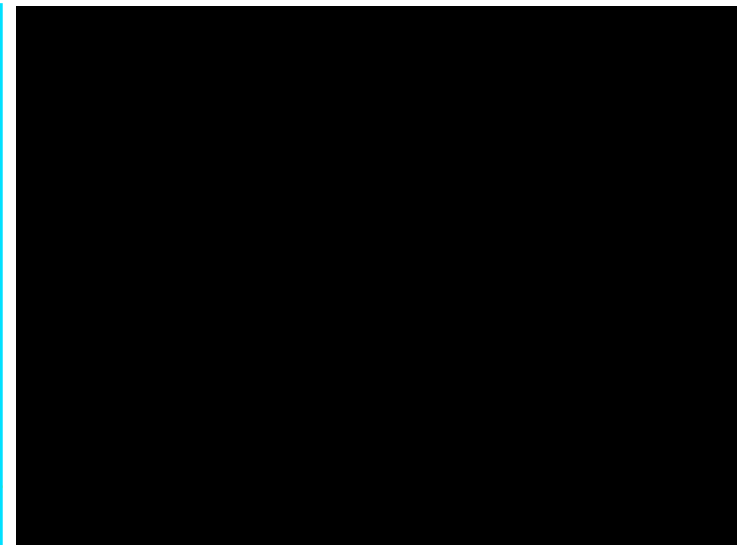
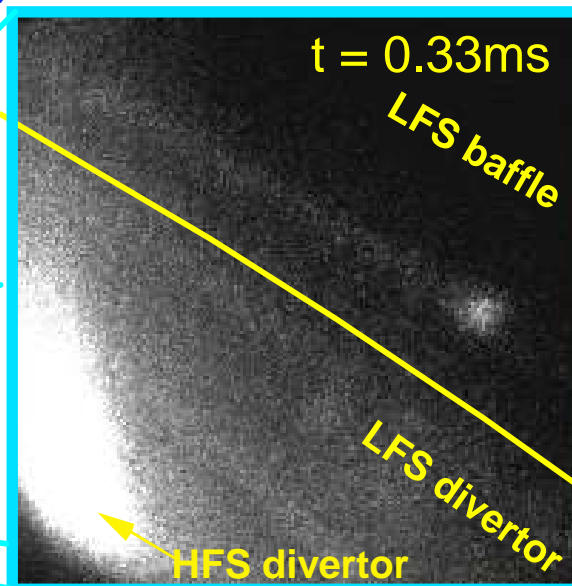


Particle flux is deposited locally, but extended over wide area: LFS baffle as well as divertor plate

(512x1025 pixels, 3kHz)



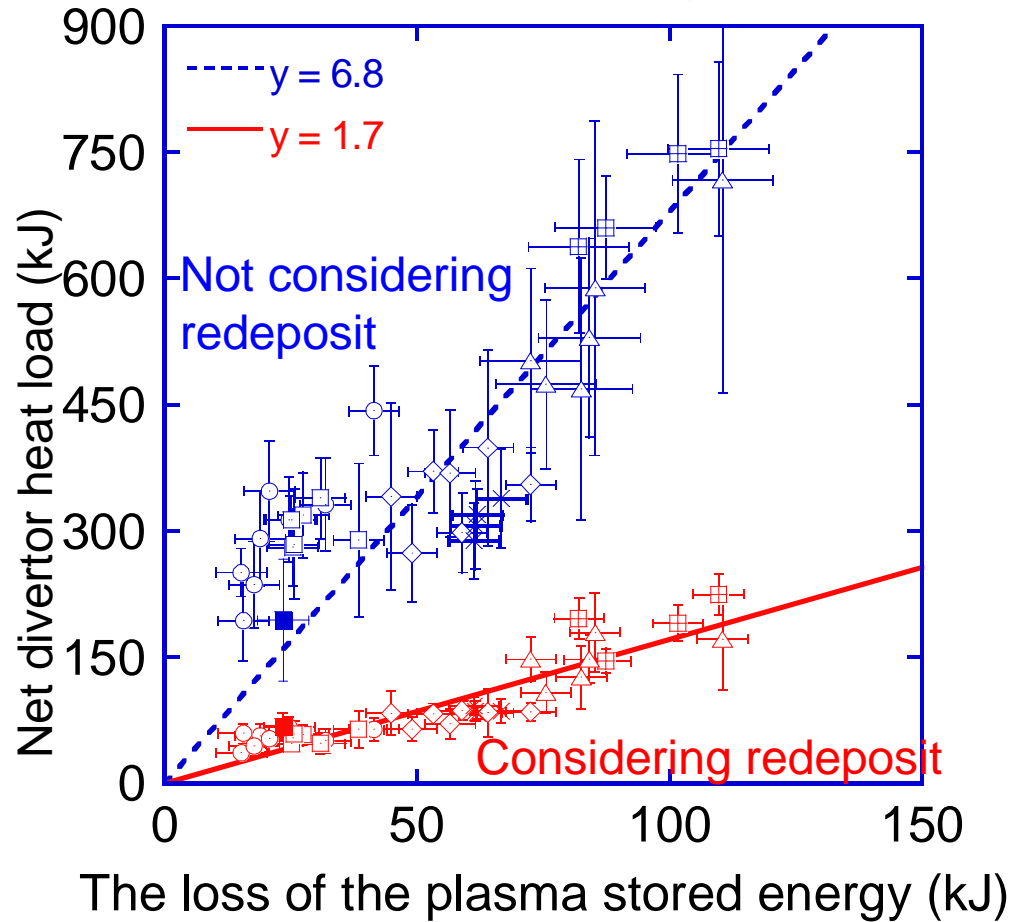
(512x512 pixels, 6kHz)



↑ ↑↑ ELMs

# Application to estimation of ELMs heat loads

Net divertor heat loads estimated from the IR-camera as a function of the loss of the stored energy by ELMs.



- Thermal properties of the outer divertor are assumed to be equal to those of CFC.
- On the inner divertor, heat loads decrease to 10% taking account of the redeposition layer.
- The total heat loads used to be estimated as 6.8 times the loss of the stored energy.
- ELMs heat loads should be smaller than the loss of the stored energy.
- The difference between the heat loads and the loss becomes smaller taking account of thermal properties of the layer on the inner divertor, whereas estimated heat loads are still 1.7 times the loss.

This is probably caused by

- the poloidal distribution of the thermal properties
- heat flux asymmetry inherent in the device (alignment of tiles or position of heating systems...).

